

## Axial and lateral particle ordering in finite Reynolds number channel flows

Katherine J. Humphry,<sup>1,a)</sup> Pandurang M. Kulkarni,<sup>2,b)</sup> David A. Weitz,<sup>1,3</sup> Jeffrey F. Morris,<sup>2</sup> and Howard A. Stone<sup>3,c)</sup>

<sup>1</sup>*Department of Physics, Harvard University, Cambridge, Massachusetts 02138, USA*

<sup>2</sup>*Department of Chemical Engineering and Benjamin Levich Institute, The City College of New York, New York, New York 10031, USA*

<sup>3</sup>*School of Engineering and Applied Sciences, Harvard University, Cambridge, Massachusetts 02138, USA*

(Received 25 April 2010; accepted 21 July 2010; published online 18 August 2010)

Inertial focusing in a pressure-driven flow refers to the positioning of particles transverse to the mean flow direction that occurs as a consequence of a finite particle Reynolds number. In channels with rectangular cross-sections, and for a range of channel aspect ratios and particle confinement, experimental results are presented to show that both the location and the number of focusing positions depend on the number of particles per unit length along the channel. This axial number density is a function of both the channel cross-section and the particle volume fraction. These results are rationalized using simulations of the particle-laden flow to show the manner in which hydrodynamic interactions set the preferred locations in these confined flows. A criterion is presented for the occurrence of a stepwise transition from one to two or more trains of particles.

© 2010 American Institute of Physics. [doi:10.1063/1.3478311]

At small but finite particle Reynolds numbers, particles in a well-established pipe flow migrate across streamlines to specific positions in the channel or tube cross-section.<sup>1–8</sup> Such focusing of particles is a consequence of inertia and was first observed in channels with a circular cross-section, where the particles migrate to an annular region approximately three-fifths of the radius from the center.<sup>1</sup> In this geometry, the underlying mechanisms have been studied extensively, and particle focusing is understood to arise from the force balance between a wall effect that pushes the particles toward the center of the channel and a shear-gradient-induced migration that pushes particles toward the boundary.<sup>9–12</sup> More recently, inertial focusing has been observed in channels with square and rectangular cross-sections, where the particle size often approaches the dimensions of the channel cross-section.<sup>6–8,13,14</sup> Because this phenomenon localizes the particles to specific positions, it has been used for separation, filtration, and improved encapsulation efficiencies, and has the potential for incorporation into microfluidic lab-on-a-chip technologies.<sup>6–8,15</sup> While the focusing positions and particle ordering in these confined, rectangular cross-sections have been described<sup>6–8,14</sup> and the lift force on particles in square cross-section channels has been investigated,<sup>13</sup> questions remain. In particular, consequences of the combination of confining geometries, inertia, and particle concentration have not been characterized.

Given the intense interest in the application of microfluidic approaches for manipulating particles and cells, there is a need to develop prediction methods based on understanding the basis of this inertially modulated ordering. To address

this need, in this letter, we study the effects of particle concentration and channel geometry on inertial focusing in microfluidic channels with rectangular cross-sections. We find that both the location and the number of focusing positions depend on the number of particles per unit length along the channel, which is a function of both the channel cross-section and particle volume fraction. Finally, we present a model in the form of a scaling law for the transitions in observed particle ordering and rationalize the results using numerical simulations to characterize the hydrodynamic interactions.

We fabricate 6 cm long microfluidic channels in poly(dimethylsiloxane) using standard soft-lithography techniques.<sup>16</sup> The channels have a rectangular cross-section that remains constant along the length of the channel. Polystyrene beads (Duke Scientific) with diameter  $d=9.9\ \mu\text{m}$  are dispersed in water with 0.1% w/v of polyethylene glycol sorbitan monolaurate (Tween 20, Sigma-Aldrich) to prevent aggregation. The particles are density matched with an aqueous solution of iodixanol (Optiprep, Sigma-Aldrich) so that the density  $\rho=1.05\ \text{g/cm}^3$  and the dynamic viscosity  $\eta\approx 1\ \text{cP}$ . The resulting suspension is loaded into a 1 ml glass syringe (Hamilton) and flowed through the microfluidic channel at constant flow rate,  $q$ , using a syringe pump (Harvard Apparatus). To observe the positions of the beads, we use a high-speed camera (Vision Research) mounted on an inverted optical microscope (Leica).

Although the particles are initially located randomly within the channel cross-section, they migrate in the directions transverse to the flow and assume characteristic focusing positions and spacings, as shown schematically in Figs. 1(a)–1(c). The behavior is shown for a range of particle volume fractions  $\phi$  and channel widths  $w$  in Figs. 1(d)–1(f). The channel height  $h=25\ \mu\text{m}$  and average flow speed  $u=0.3\ \text{m/s}$  are fixed so that the experiments show the influence of changing the aspect ratio of the channel cross-

<sup>a)</sup>Electronic mail: katie.humphry@shell.com. Present address: Projects and Technology, Shell International B.V., 2288 GS Rijswijk, The Netherlands.

<sup>b)</sup>Present address: Department of Chemical Engineering, University of California, Santa Barbara, CA 93106, USA.

<sup>c)</sup>Present address: Department of Mechanical and Aerospace Engineering, Princeton University, Princeton, NJ 08544, USA.

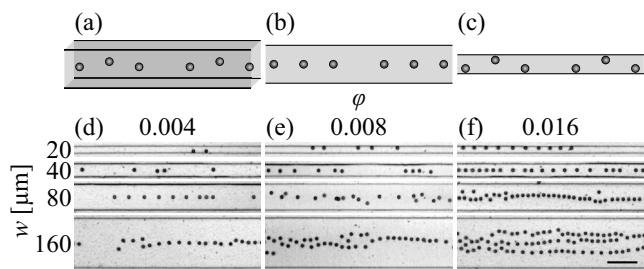


FIG. 1. [(a)–(c)] Schematics showing typical particle positions in a rectangular channel after inertial focusing. (a) Three-dimensional projection. (b) Projection of (a) onto the longer channel wall. (c) Projection of (a) onto the shorter channel wall. [(d)–(f)] Images illustrating inertial ordering in rectangular channels for a range of channel widths,  $w$ , and bead volume fractions,  $\phi$ , at the end of a 6 cm long channel with height  $h=25 \mu\text{m}$ . The flow rate is adjusted to achieve the same average flow speed,  $u=0.3 \text{ m/s}$ . Flow is from left to right. Volume fractions: (d)  $\phi=0.004$ , (e)  $\phi=0.008$ , and (f)  $\phi=0.016$ . Scale bar= $100 \mu\text{m}$ . For  $w=40, 80, 160 \mu\text{m}$  channel perspective is as in (b). For  $w=20 \mu\text{m}$  channel perspective is as in (c).

section. The Reynolds number,  $\text{Re}=uD/\nu=[6.7, 10.7]$ , where  $D=(2wh)/(w+h)$  is the hydraulic diameter of the channel and  $\nu$  is the kinematic viscosity. The particle Reynolds number,  $\text{Re}_p=\text{Re}(d/D)^2$ , falls in the range  $[0.8, 1.3]$ .

The images shown in Figs. 1(d)–1(f) illustrate several phenomena. First, particles focus to the center of the longer dimension of the channel and to either side of the centerline in the short dimension, as previously reported.<sup>7</sup> Second, trains of particles with regular spacing are observed in the axial flow direction (here  $x$ ), again in agreement with previous reports.<sup>5–7,17</sup> Third, we find that there is a systematic increase in the number of rows of ordered particles in the lateral direction ( $y$ ), as  $\phi$  or  $w$  increases.

To quantify the particle ordering in both the axial and lateral directions, we define a relative occupancy function,  $p(\mathbf{r})$ , determined by building a histogram for the location of all neighbors around each reference particle and normalizing by the bin size. The resulting function is normalized to the maximum for each condition by dividing by the largest value. The centers of the particles are found using customized tracking routines.<sup>18</sup> Plots of  $p(\mathbf{r})$  for several  $\phi$  in a channel of  $w=160 \mu\text{m}$  and  $h=25 \mu\text{m}$  illustrate the tendency for the formation of more trains when the number of particles within a section of the channel increases (Fig. 2). Each of these  $p(\mathbf{r})$  represents data from at least 700 individual particles. Local maxima in the  $p(\mathbf{r})$  indicate the most probable particle center spacings. Note that the  $p(\mathbf{r})$  are for a two-dimensional projection.

We observe that  $p(\mathbf{r})$  exhibits maxima in both the lateral and axial directions (Fig. 2). The maxima in the axial direction indicate the most often observed center-to-center particle spacing in the direction of flow. As one moves along the  $x$ -axis from left to right, the peaks indicate the distance in the flow direction to nearest neighbors at separation  $\ell$ , second nearest neighbors at roughly  $2\ell$ , and so on. The positions of these peaks do not change appreciably as  $\phi$  increases. The number of maxima in the  $y$ -direction indicates the number of particle trains,  $m$ , in the lateral direction. We find a systematic increase in  $m$  as  $\phi$  increases, as shown by Figs. 1(d)–1(f) and 2. The variation of  $m$  with  $\phi$  is shown in Fig. 3(a). In this

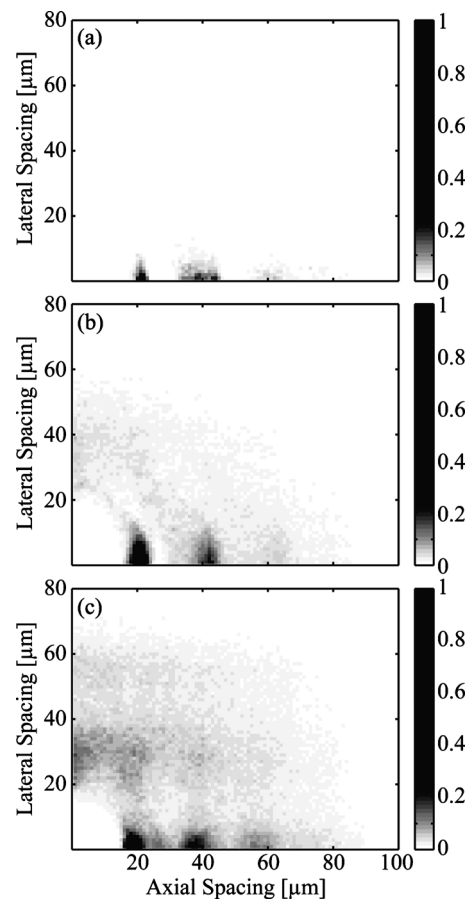


FIG. 2. A grayscale map illustrating  $p(\mathbf{r})$  for  $9.9 \mu\text{m}$  diameter beads in channels with width  $w=160 \mu\text{m}$  and height  $h=25 \mu\text{m}$  as measured at the end of a 6 cm long channel. The flow rate,  $q=64 \mu\text{l/min}$ , corresponds to an average flow speed,  $u=0.3 \text{ m/s}$ . The volume fractions are (a)  $\phi=0.004$ , (b)  $\phi=0.008$ , and (c)  $\phi=0.016$ . [(a)–(c)] correspond to Figs. 1(d)–1(f), respectively. The values of  $p(\mathbf{r})$  are normalized so that maximum value in each grayscale map is equal to one.

system  $\phi=\lambda(\pi d^3/6wh)$ , where  $\lambda$  is the axial number density, i.e., the number of particles per unit length in the  $x$ -direction.

We postulate that at sufficiently low  $\phi$ , only a single particle train is present. This occurs when  $\lambda$  is sufficiently low, namely, when  $\lambda < 1/\ell$ . As  $\lambda$  increases, a point is reached where another bead cannot be added to the single particle train, while still maintaining the preferred axial spacing,  $\ell$ , and thus a second bead train is formed. If this hypothesis is correct, then a transition from one bead train to two should occur when  $1/\lambda=\ell$  or  $\lambda d=d/\ell=6\phi wh/\pi d^2$ . Similarly, there should be a transition from two bead trains to three when  $6\phi wh/\pi d^2=2d/\ell$ . In general, an increase in the number of bead trains from  $m$  to  $m+1$  is expected to occur when

$$\frac{6\phi wh}{\pi d^2} = \frac{md}{\ell}, \quad (1)$$

where  $m$  is a positive integer.

We plot the number of bead trains in the lateral direction as a function of  $6\phi wh/\pi d^2$  in Fig. 3(b). The number of bead trains in the lateral directions increases from 1 to 2 around  $6\phi wh/\pi d^2=0.5$  and from 2 to 3 around  $6\phi wh/\pi d^2=1$ , in agreement with the criterion presented in Eq. (1) with

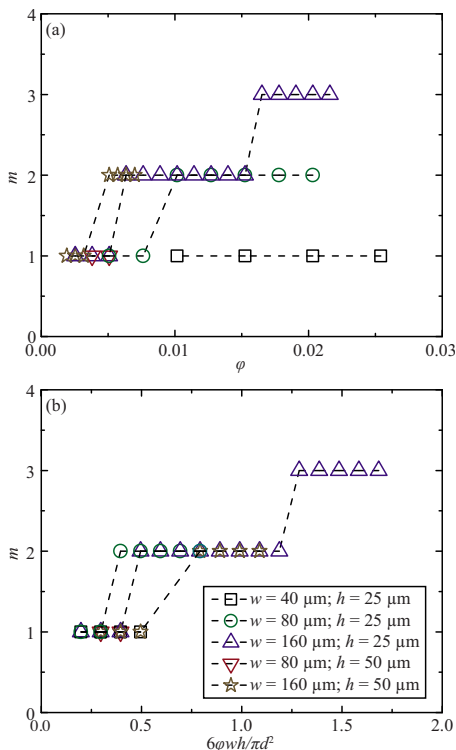


FIG. 3. (Color online) Number of bead trains in the lateral direction,  $m$ , as a function of (a)  $\phi$  and (b)  $6\phi w h / \pi d^2$ . Particles are flowing in channels with heights  $h=25$  and  $50 \mu\text{m}$  and widths  $w=40$ ,  $80$ , and  $160 \mu\text{m}$ . Data are taken at the end of a  $6 \text{ cm}$  long channel. Dashed lines included as a guide for the eye. Note that the three transitions from one to two beads indicated in (a) span almost an order of magnitude in  $\phi$ , while the reduced linear number density shown in (b) brings the transitions to within a factor of 2 of each other.

$\ell \approx 2d$ . This result allows for substantially better collapse of data for channels with different cross-section.

Next, we determine the average axial spacing  $\ell$  as a function of  $\phi$  for a range of channel cross-sections in Fig. 4(a). The axial spacing does not depend strongly on channel cross-section or on the volume fraction, and  $\ell \approx 22 \mu\text{m} \approx 2.2d$  [Fig. 4(a)]. Values of  $\ell$  have previously been reported for other experimental conditions: in cylindrical tubes<sup>5</sup> with  $d=[1/17, 1/33]D$  values of  $\ell$  in the range  $[2.4, 4.5]d$  ( $\ell$  decreasing as  $\text{Re}_p$  increases) were reported for  $\text{Re}_p \approx 1$ ; rectangular channels<sup>7</sup> with cross-section of  $27 \times 52 \mu\text{m}^2$  and  $\text{Re}_p = 0.4$  yielded  $\ell = 2.5d$  with  $d = 9.9 \mu\text{m}$ ; and square channels<sup>6</sup> with cross-section of  $50 \times 50 \mu\text{m}^2$  and  $\text{Re}_p = 3.1$  yielded  $\ell = 3.6d$  for  $d = 10 \mu\text{m}$ . The values of  $\ell$  found here agree with the values reported for rectangular channels.<sup>7</sup>

To examine the physical mechanisms underlying the observed regular axial spacing, we perform numerical simulations at finite  $\text{Re}$  in a wall-bounded geometry using the lattice Boltzmann method.<sup>19,20</sup> First, we compute the steady disturbance flow around an isolated particle. A particle size of  $d=24$  lattice units is chosen and the size of the computational box is  $10d \times 4d \times 2.5d$ . We implement no-slip at the walls and periodicity in the flow direction. Pressure-driven flow is imposed by applying the same steady force density at each lattice node.<sup>19</sup> The particle starts from an arbitrary location in the cross-section and migrates to its equilibrium location at the center of the longer side, and is displaced

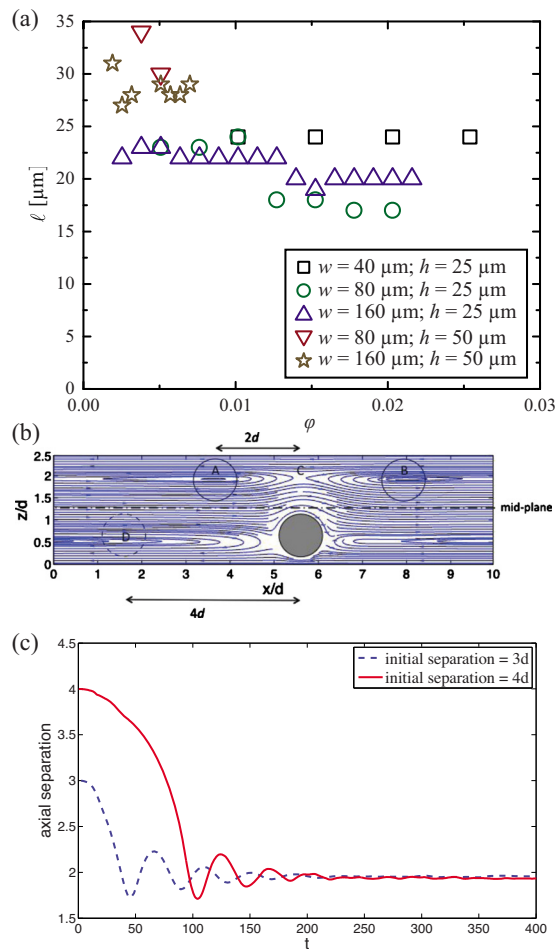


FIG. 4. (Color online) (a) Experimentally measured average distance in the direction of flow to the nearest particle as a function of volume fraction,  $\phi$ , in channels with heights  $h=25$  and  $50 \mu\text{m}$  and widths  $w=40$ ,  $80$ , and  $160 \mu\text{m}$ . Data are taken at the end of channels with length  $L=6 \text{ cm}$ . The average flow speed is  $u=0.3 \text{ m/s}$  for all data shown. (b) Streamlines around an isolated particle in the  $xz$  plane computed using lattice Boltzmann simulations. The solid and dotted circles suggest positions of adjacent particles. (c) Axial separation for spheres at the equilibrium relative to both walls as a function of time made dimensionless by dividing by  $w/2u$ , as computed by the lattice Boltzmann method.

from the centerline in the short dimension (see Fig. 1). In Fig. 4(b), we plot, for  $\text{Re}_p=1.25$ , the steady streamlines in a frame moving with the particle center in the  $xy$ -plane passing through the midline of the longer channel wall.

The streamline structure in the vicinity of the particle [Fig. 4(b)] is similar to that for simple shear flow at  $\text{Re}_p=O(1)$ .<sup>21–23</sup> It is characterized by open and reversing streamline regions with the addition of a near-field spiraling region. The small dimensions of the channel allow a particle in one-half to disturb the flow in the other half of the channel. This results in two inward spiraling regions, centered at A and B, on either side of the particle, and a saddle point indicated by C.

In the case of a simple shear flow, it has been shown that the trajectories of a second particle are qualitatively similar to the streamlines around a single particle in both Stokes<sup>24</sup> and finite-Reynolds-number flows.<sup>21</sup> It is therefore expected that in a fully developed flow, a second neighboring particle would migrate to the center of spirals generated by the first

particle. This observation suggests that nearest neighbor particles [shown by open circles in Fig. 4(b)] should be centered at points A and B, setting  $\ell \approx 2d$ . Note that the adjacent particle will subsequently disturb the flow lines, favoring the positioning of a third particle at location D, at an axial separation of approximately  $2l \approx 4d$ . We have performed computations for channel dimensions of  $6d \times 3d$  and found that  $\ell \approx 2.25d$  for this case, suggesting that  $\ell$  increases as the particles are less confined.

To further support our argument that hydrodynamic interactions set  $\ell$ , we simulate the motion of a pair of spheres that are initially separated by a range of distances in the flow direction but located roughly at their inertial focusing equilibrium points with respect to the channel walls. While not addressed here, the axial distance required to reach this configuration scales as  $\text{Re}_p^{-1}$  and is addressed in other works.<sup>25</sup> Figure 4(c) shows the axial spacing between the pair as a function of dimensionless time  $ut/h$  for two initial separations. The pair approaches on a damped oscillatory trajectory and eventually reaches a steady axial spacing of  $\ell = 1.95d$ ; the form of the trajectory depends on the channel dimensions as the oscillations are less pronounced for the same  $\text{Re}$  in a  $6d \times 3d$  channel. The computed steady separation compares favorably with our experimental measurements. Note that in Stokes flow, reversibility implies that relative trajectories are set by the initial condition. As a consequence, for the conditions of Fig. 4(c), the Stokes trajectory would either execute a periodic motion or the separation distance must vary monotonically with time. Motion to a specific location is thus a result of inertia. This result is true even if the structure of the streamlines is largely similar to that in Stokes flow within the geometry; this is the case here as the flow relative to a single particle at  $\text{Re} \rightarrow 0$  is visually similar with reversing zones,<sup>26</sup> although the spiraling is apparently due to inertia. With axial spacing set by hydrodynamic interactions, the physical mechanism underlying the number of particle trains in the lateral direction, as presented in Eq. (1), is better illuminated.

In conclusion, we have probed the effects of inertia, at low but finite particle Reynolds numbers, and particle concentration in confining channels with rectangular cross-section. We observe multiple parallel trains of particles. Investigation of the influence of the channel cross-section and particle volume fraction results in a criterion that predicts the number of particle trains. We find that the axial spacing for inertially focused particles is similar to that reported in previous experiments that cover a range of channel cross-sections.<sup>5-7</sup> Furthermore, we use simulations to investigate the mechanism underlying this regular spacing and find that confinement in the channel leads to fixed points in the flow with respect to the particle, and these roughly define the positions of neighboring particles in the axial direction. Inertially influenced hydrodynamic interaction is thus the mechanism for the appearance of multiple particle trains as concentration is increased.

This work was supported by the Harvard MRSEC (Grant No. DMR-0820484) and NSF Grant No. 0853720 (J.F.M.). Computations were performed at the CUNY High Perfor-

mance Computing Facility at the College of Staten Island. We thank J. Edd and D. Di Carlo for useful discussions.

- <sup>1</sup>G. Segré and A. Silberberg, "Radial particle displacements in Poiseuille flow of suspensions," *Nature (London)* **189**, 209 (1961).
- <sup>2</sup>R. C. Jeffrey and J. R. A. Pearson, "Particle motion in laminar vertical tube flow," *J. Fluid Mech.* **22**, 721 (1965).
- <sup>3</sup>D. Walz and F. Grün, "The radial velocity of spherical particles in tubular pinch effect experiments," *J. Colloid Interface Sci.* **45**, 467 (1973).
- <sup>4</sup>B. P. Ho and L. G. Leal, "Migration of rigid spheres in a two-dimensional unidirectional shear flow of a second-order fluid," *J. Fluid Mech.* **76**, 783 (1976).
- <sup>5</sup>J. P. Matas, V. Glezer, E. Guazzelli, and J. F. Morris, "Trains of particles in finite-Reynolds-number pipe flow," *Phys. Fluids* **16**, 4192 (2004).
- <sup>6</sup>D. Di Carlo, D. Irimia, R. G. Tompkins, and M. Toner, "Continuous inertial focusing, ordering, and separation of particles in microchannels," *Proc. Natl. Acad. Sci. U.S.A.* **104**, 18892 (2007).
- <sup>7</sup>J. F. Edd, D. Di Carlo, K. J. Humphry, S. Köster, D. Irimia, D. A. Weitz, and M. Toner, "Controlled encapsulation of single-cells into monodisperse picolitre drops," *Lab Chip* **8**, 1262 (2008).
- <sup>8</sup>A. A. Bhagat, S. S. Kuntaegowdanahalli, and I. Papautsky, "Enhanced particle filtration in straight microchannels using shear-modulated inertial migration," *Phys. Fluids* **20**, 101702 (2008).
- <sup>9</sup>P. G. Saffman, "The lift on a small sphere in a slow shear flow," *J. Fluid Mech.* **22**, 385 (1965).
- <sup>10</sup>R. G. Cox and H. Brenner, "The lateral migration of solid particles in Poiseuille flow—I. Theory," *Chem. Eng. Sci.* **23**, 147 (1968).
- <sup>11</sup>J. A. Schonberg and E. J. Hinch, "Inertial migration of a sphere in Poiseuille flow," *J. Fluid Mech.* **203**, 517 (1989).
- <sup>12</sup>E. S. Asmolov, "The inertial lift on a spherical particle in a plane Poiseuille flow at large channel Reynolds number," *J. Fluid Mech.* **381**, 63 (1999).
- <sup>13</sup>D. Di Carlo, J. F. Edd, K. J. Humphry, H. A. Stone, and M. Toner, "Particle segregation and dynamics in confined flows," *Phys. Rev. Lett.* **102**, 094503 (2009).
- <sup>14</sup>B. Chun and A. J. C. Ladd, "Inertial migration of neutrally buoyant particles in a square duct: An investigation of multiple equilibrium positions," *Phys. Fluids* **18**, 031704 (2006).
- <sup>15</sup>D. Di Carlo, J. F. Edd, D. Irimia, R. G. Tompkins, and M. Toner, "Equilibrium separation and filtration of particles using differential inertial focusing," *Anal. Chem.* **80**, 2204 (2008).
- <sup>16</sup>D. C. Duffy, C. J. McDonald, O. J. A. Schueller, and G. M. Whitesides, "Rapid prototyping of microfluidic systems in poly(dimethylsiloxane)," *Anal. Chem.* **70**, 4974 (1998).
- <sup>17</sup>G. Segré and A. Silberberg, "Behaviour of macroscopic rigid spheres in Poiseuille flow. Part 2. Experimental results and interpretation," *J. Fluid Mech.* **14**, 136 (1962).
- <sup>18</sup>J. C. Crocker and D. G. Grier, "Methods of digital video microscopy for colloidal studies," *J. Colloid Interface Sci.* **179**, 298 (1996).
- <sup>19</sup>A. J. C. Ladd and R. Verberg, "Lattice-Boltzmann simulations of particle-fluid suspensions," *J. Stat. Phys.* **104**, 1191 (2001).
- <sup>20</sup>C. K. Aidun, Y. Lu, and E. J. Ding, "Direct analysis of particulate suspensions with inertia using the discrete Boltzmann equation," *J. Fluid Mech.* **373**, 287 (1998).
- <sup>21</sup>P. M. Kulkarni and J. F. Morris, "Pair-sphere trajectories in finite-Reynolds-number shear flow," *J. Fluid Mech.* **596**, 413 (2008).
- <sup>22</sup>D. R. Mikulencak and J. F. Morris, "Stationary shear flow around fixed and free bodies at finite Reynolds number," *J. Fluid Mech.* **520**, 215 (2004).
- <sup>23</sup>G. Subramanian and D. L. Koch, "Centrifugal forces alter streamline topology and greatly enhance the rate of heat and mass transfer from neutrally buoyant particles to a shear flow," *Phys. Rev. Lett.* **96**, 134503 (2006).
- <sup>24</sup>G. K. Batchelor and J. T. Green, "The hydrodynamic interaction of two small freely-moving spheres in a linear flow field," *J. Fluid Mech.* **56**, 375 (1972).
- <sup>25</sup>P. M. Kulkarni, "Suspension mechanics at finite inertia," Ph.D. thesis, City University of New York, 2009.
- <sup>26</sup>M. Zurita-Gotor, J. Bławdziewicz, and E. Wajnryb, "Swapping trajectories: A new wall-induced cross-streamline particle migration mechanism in a dilute suspension of spheres," *J. Fluid Mech.* **592**, 447 (2007).